

Original Article

# Investigation of The Effect of Elastic Modulus of Material for Ballasted Railway Double Railway Track Using Numerical Analysis

Nirmal Chandra Roy<sup>1,2</sup>, Md. Abu Sayeed<sup>2</sup>

<sup>1</sup>Department of Civil Engineering, Hajee Mohammad Danesh Science and Technology University, Dinajpur, Bangladesh.

<sup>2</sup>Department of Civil Engineering, Rajshahi University of Engineering and Technology, Rajshahi, Bangladesh.

<sup>1</sup>Corresponding Author : [ncr.civil@hstu.ac.bd](mailto:ncr.civil@hstu.ac.bd)

Received: 11 October 2025

Revised: 15 November 2025

Accepted: 12 December 2025

Published: 29 December 2025

**Abstract** - Railways have been the preferred means of public transit as highway traffic congestion has increased, leading to a global demand for quicker and heavier trains. However, single-track railway systems are usually unable to meet these growing demands. Double-track railroad systems were constructed in order to get around this problem. Significant vibrations are caused in the railway track system by high-speed trains and large axle loads, which increases the danger of track damage and catastrophe. The behavior of ballasted double-track foundations at various speeds must be thoroughly understood in order to improve the safety and operational dependability of high-speed trains. This study performs a Three-Dimensional (3D) numerical simulation to assess the dynamic response of ballasted double-track railway systems under high-speed train loads. Key design parameters influencing track performance are also examined. The results are analyzed, visualized, and their practical implications for high-speed railway design and maintenance are discussed. Finally, regression analysis revealed that a strong linear relationship is found between the mean displacement and modulus of elasticity of materials ( $R=0.962$ ), and between distance and displacement ( $R=0.869$  to  $0.974$ ) for three different moduli of elasticity.

**Keywords** - Ballasted double railway track, Displacement, High-Speed Trains, Numerical Modelling, Traffic congestion.

## 1. Introduction

Rapid growth in urban populations has led to severe congestion in metropolitan road networks. Traffic congestion is considered highly disagreeable, as it imposes substantial direct expenses on both the economy and road users through delays and reduced mobility. According to the INRIX Global Traffic Scorecard (2023), traffic congestion in the United States alone causes annual economic losses ranging from \$150 billion to \$200 billion [1]. Furthermore, congestion increases greenhouse gas emissions due to excess fuel consumption, thereby exacerbating global warming and contributing to climate change [2]. Because of these drawbacks, railroads are now the most popular form of public transportation, especially for long-distance travel and heavy freight transportation. Improved environmental sustainability, cost-effectiveness, and dependability are some of their advantages. By offering quicker and greener substitutes for conventional transit systems, High-Speed Trains (HSTs) have revolutionized contemporary travel. However, track infrastructure is severely strained by the introduction of high-speed trains and massive axle weights, especially dynamic loading, which results in excessive vibrations. Train stability, track foundation degradation, rail fatigue damage, and likely electrical system

disruptions are all exacerbated by these dynamic effects [3]. Because of their stability, drainage ability, and ease of maintenance, ballasted railway tracks remain the most widely used track structure. A typical ballasted track consists of a substructure and a superstructure. The sleepers, which are buried in the ballast layer, receive wheel loads from the rails. In order to reduce stress transmission into the sub-grade, the ballast disperses these loads over a larger area [4]. For long-term performance and to avoid subgrade failure, the ballast and sub-ballast layers' thickness and compaction are essential. The complex interactions among all the components of the track control the dynamic manners of ballasted tracks. The ballast layer anchors the track shape, facilitates drainage, and absorbs dynamic train-induced loads, among other functions [5]. Nevertheless, track stability and serviceability are reduced due to the breakage and compaction of ballast particles [6]. Track performance and load distribution are improved by properly graded and compacted ballast [7, 8]. One major problem that impacts ballast performance is ballast fouling. This happens when small particles like sand or clay seep into the ballast, reducing its porosity and drainage capacity. Fouling increases the likelihood of track settling during cyclic stress by decreasing ballast resilience, according to Liu et al.



[9]. Therefore, it is essential to comprehend the track's dynamic feedback with the purpose of preventing deformation-related problems like ballast degradation, sleeper displacement, and rail deflection [10]. As the number of freight cycles rises, the resilient modulus, a measure of ballast elasticity under repeated loads, declines, leading to cumulative, irreversible deformations [11]. Unsafe operating conditions and misalignment result from excessive settlement (Fischer S., 2024). Settlement rates and maintenance intervals are also impacted by variables like ballast shape, subgrade stiffness, and fastening quality. Routine procedures to restore track quality include tamping, cleaning, and replacing ballast; however, incorrect tamping can worsen ballast degradation [12]. Depending on traffic volumes and exposure to the environment, ballast usually needs to be completely replaced every ten to fifteen years [13]. Ballasted track performance is greatly impacted by geotechnical and environmental factors. Track behavior is significantly influenced by temperature, moisture content, and subgrade quality. Saturated or weak subgrades accelerate ballast degradation and worsen deformation [14]. Techniques like soil stabilization and geotextile reinforcement are frequently used to address these problems. Wet weather increases the risk of settlement and further jeopardizes ballast stability [15]. Novel strategies to enhance ballast performance have been investigated in recent studies. It has been demonstrated that recycled materials, such as crushed concrete or rubber granules, provide comparable structural advantages while lowering expenses and environmental effects [16]. Furthermore, because of their capacity to improve load distribution, lessen settlement, and stop fouling and lateral migration of ballast particles, geosynthetics, such as geogrids and geotextiles, are becoming more and more popular [17]. Train-track-ground interaction has been simulated using a variety of computational techniques, for instance, the Boundary Element (BE) method [21], the Finite Element (FE) method [18-20], and 2.5D FE-BE hybrid approaches [22-25]. Ballast behaviour under long-term cyclic compression was further studied using boundary surface plasticity models, demonstrating the complexity of the ballast degradation under repeated loading according to Rahman et al [26]. Computational modelling has evolved from simplified 2D assumptions to 3D finite element and DEM. Recent hybrid FE-DEM studies demonstrated improved accuracy in predicting ballast breakage and stress transfer mechanisms [27]. The investigation of the stress circulation in the ballast and subgrade layers under dynamic train loading conditions has shown that 3D FE modelling is the most effective of these. The behaviour of double-track railway foundations under dynamic moving loads has not been thoroughly studied, despite the fact that single-track ballasted systems have been the subject of much research. The few studies that are currently available focus mostly on train track interaction without taking into account the combined impacts of concurrent loads from nearby tracks. There is an urgent need to look into double-track railway systems that can handle the demands of contemporary transportation, even though the

majority of modelling efforts concentrate on single-track railways, which have drawbacks like low capacity, delays, and rigidity. There has been little prior research on 3D FE modelling for double-track railroads [28, 29], and there are still a lot of unanswered questions because there isn't enough verified field data. This emphasizes how important it is to create sophisticated 3D finite element models in order to faithfully replicate failure mechanisms and behaviour in the real world. This study's primary goals are to: i) Create a validated 3D Finite Element (FE) numerical model for analysing and forecasting how ballasted double-track railway foundations will behave under dynamic moving loads. ii) To look into how material characteristics impact ballasted double-track systems' performance.

## 2. Methods and Materials

A three-dimensional FE model was advanced to predict the dynamic behavior of a ballasted double-track railway system exposed to high-speed loading. The model was implemented using the Midas-GTS NX commercial program [30]. The numerical simulation allows for the interplay between track components and the underlying soil foundation, and captures stress distribution, displacement response, and vibration patterns under various loading scenarios.

### 2.1. Model Validation

A rigorous validation approach is utilized to determine the 3D FEM's correctness and dependability. The historical temporal responses of sleeper deformation during train passing periods were utilized to confirm the modeling of the X-2000 HST railway system in Ledsgard, just outside Göteborg. A three-dimensional model of the railway track system is created, and all the materials data is imported. Then, the dynamic load of the train is generated using FEM, and an analysis is performed to check the model validation.

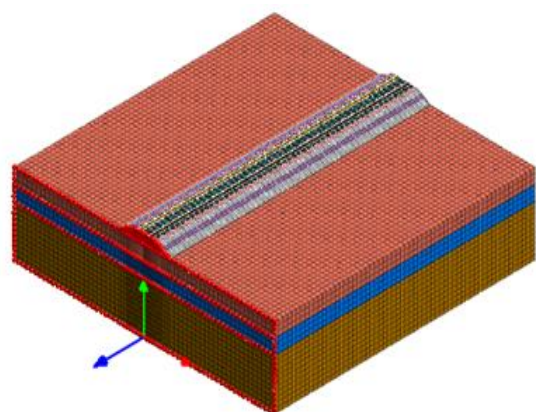


Fig. 1 3D View of ballasted railway track for validation

Figure 1 shows the 3D view of the railway system of that site. At the track's middle point, the Midas GTS NX application computes the period-history reactions of the sleeper deformation for a speed of 70 km/h.

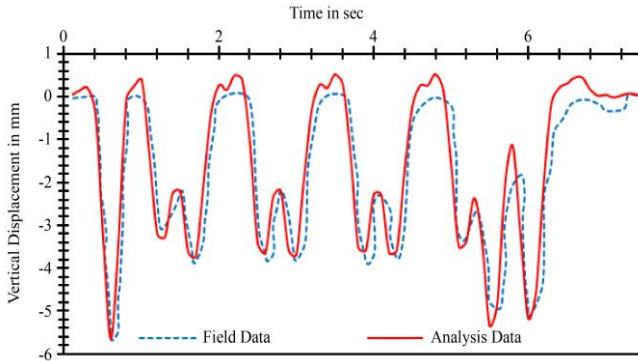


Fig. 2 Comparison of field observations with fe estimated data responses at the track center

The simulation data were linked with corresponding field data obtained at a train speed of 70 km/h, as depicted in Figure 2. Although minor discrepancies are observed between the field data and simulation data, the comparison confirms that the numerical model effectively captures the vertical displacement behavior of the railway track system under dynamic loading. The consistency between the simulated and experimental data enhances the credibility and reliability of the FEM approach. To further assess model accuracy and sensitivity, statistical validation metrics were employed. The RMSE was found to be 0.6 mm, and the  $R^2$  value was 0.92, indicating a high level of correlation and excellent agreement between the numerical predictions and the field observations, which are listed in Table 1.

Table 1. Statistical analysis result

Parameter	Field Measurement	3D FEM Result	Statistical Metric	Value	Interpretation
Vertical Displacement Profile	At a 70 km/h train speed	Simulated Response	RMSE	0.6 mm	Very small average deviation
			Coefficient of Determination ( $R^2$ )	0.92	Excellent agreement, high model accuracy

## 2.2. Nominal Model

The nominal model utilized for numerical analysis has dimensions of (36m x 33m x 11m). A 2D model is built using computer-aided design software. Then, 3D meshes are created from the 2D model. A cross-sectional view of the double-lane railway track is displayed in Figure 3. The mesh size for the 3D model of the railway track structure consists of a ballast layer (0.3 m thick), sub-ballast layer (0.2 m thick), sub-grade layer (0.5 m thick), and soil layer (9.8 m deep). The total width of the double-lane track is about 10.45 m. Each track is 1.6 m wide, and a distance of 1.5 m separates the two tracks.

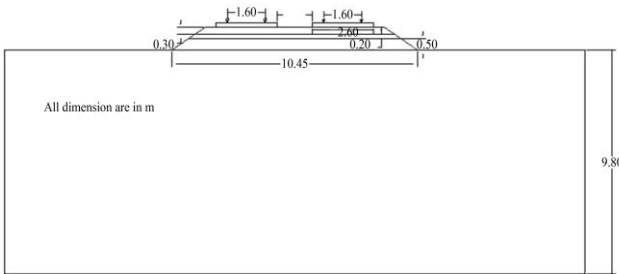


Fig. 3 2D Nominal model of the double lane railway track system

## 2.3. Material Property

Track Superstructure: Track superstructure consists of Rail, Sleeper, and Fastening system. In the model, the UIC-60 section (1D beam) is treated as a rail section element. Fasteners, which hold the rail to the sleepers, have an elastic stiffness of 100,000 kN/m. The element size of the FE model is estimated using the shortest wavelength needed to simulate high-frequency motion accurately.

Track Substructure: The track substructure is made up of different layers. The properties of sub-grade were signified as

elastic materials, whereas the ballast was modeled as an elasto-plastic Mohr-Coulomb material. A compendium of each material's attributes is provided in Table 2.

Table 2. Layer properties of the track system [31]

Layer	E (MPa)	$\mu$	$\gamma$ (kN/m <sup>3</sup> )	$\phi$	$\xi$
Ballast	400	0.10	17.7	50°	0.02
Sub-Ballast	300	0.02	21.6	40°	0.02
Sub-grade	200	0.02	21.6	36°	0.02
Soil	48	0.03	18.2	-	0.03
Sleeper	30000	0.20	20.2	-	-
Rail	210000	0.30	76.50	-	-

## 2.4. Boundary Conditions Meshing

The accuracy of FE model results depends on the mesh size and boundary conditions of the track. A denser mesh was used in high-stress zones, such as near the rails and the sleeper. The FE model mesh sizes are as follows: 0.35 m x 0.15 m x 0.15 m for sleepers and 0.5 m x 0.5 m x 0.5 m for ballast and sub-grade. A 3D model of the double-lane railway track is visualized in Figure 4.

The lateral and bottom boundaries were fully constrained to replicate semi-infinite soil conditions. To reduce reflection of dynamic waves, non-reflective dashpots were applied at the model's periphery. Viscous dampers are utilized to connect the model's lateral restrictions, simulating indefinite boundary situations and conveniently dampening incoming S- and P-waves.

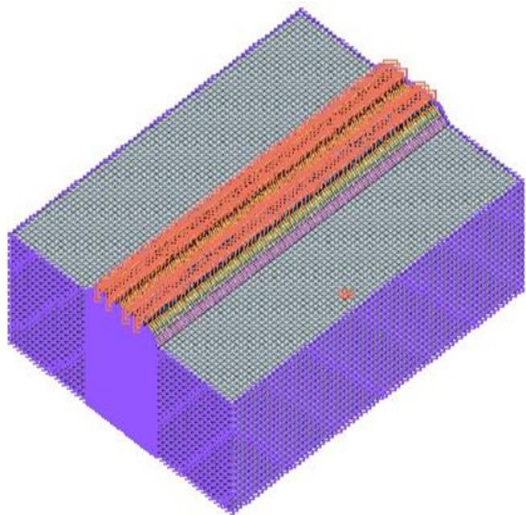


Fig. 4 3D view of the double lane railway track

### 2.5. Tarin Load Modelling

The HST moving cargo is represented by an X-2000 HST-type train in the 3D FEM. Dimensions of the X-2000 HST are modeled as in the previous study [31]. The longitudinal element size for the sleeper and rails is 0.315 m. As a result, attaching the sleeper to every other rail node ensures 0.6 m of fastener spacing. In this investigation, the Midas-GTS NX software's dynamic load capability is used to mimic a moving train load.

Figure 5 shows the dynamic weight chart for a random node with an axle force imposed on each rail.

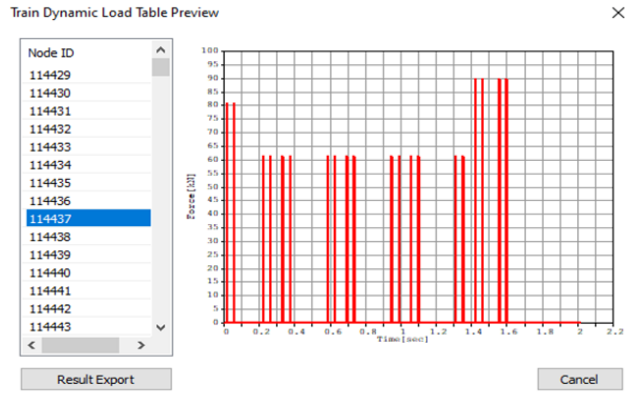


Fig. 5 Geometry of train dynamic load table for X-2000 HST

## 3. Results and Discussion

### 3.1. Investigation of the Effect of Elastic Modulus

A crucial material parameter that gauges a material's capacity to withstand deformation under stress is its elastic modulus, also known as the Modulus Of Elasticity. It has an impact on how the rails, ties (or sleepers), ballast, subgrade, and other track components behave. The aggregate elastic modulus of a railway track's constituent parts has a significant influence on how the track behaves overall when under load.

This section conducts a parametric study to investigate the impact of the elastic modulus on the lateral displacement of the rail. That is accomplished using the similar material properties (Table 1) that were discussed in the prior section. However, just the pertinent parameter varies, as shown in Table 3, to investigate a specific parameter.

Table 3. Range of variable elastic modulus for the study [32]

Parameter	Lower Value (MPa)	Nominal Value (MPa)	Upper Value (MPa)
Ballast	135	270	400
Sub-Ballast	80	135	300
Sub-grade	30	60	120

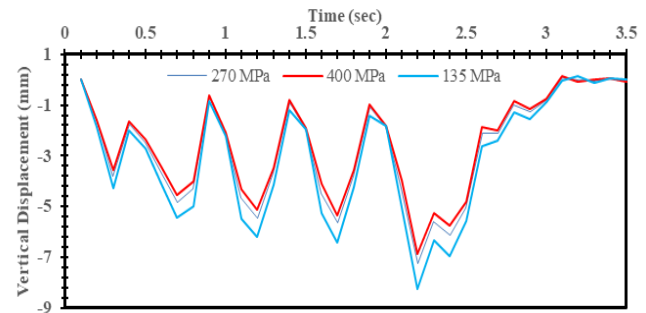


Fig. 6 Displacement of rail with various elastic moduli of ballast

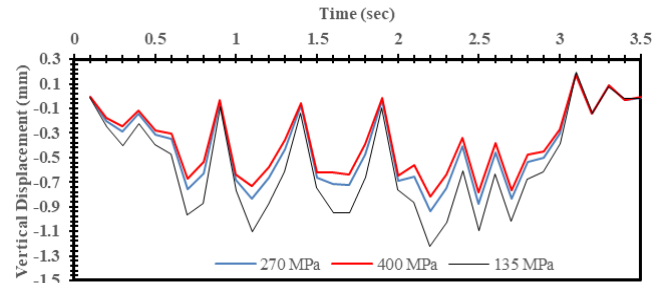


Fig. 7 Displacement of sleeper with various elastic moduli of ballast

Vertical displacement of ballasted railway track structure (rail, sleeper, ballast, sub-ballast, and sub-grade) due to different elastic moduli of ballast is shown in Figures 6 to 10. Figure 6 shows how rail displacement varies with the elastic modulus of the ballast layer over time. The graph indicates that the maximum displacement value is 8.25 mm, occurring at an elastic modulus of 135 MPa. Figure 7 illustrates the vertical displacement of the sleeper over time in relation to variations in the elastic modulus of the ballast. In the graph, the maximum displacement occurs at 135 MPa (1.22 mm), while the minimum value occurs at 400 MPa (0.82 mm). This suggests that a higher modulus of elasticity is associated with improved performance in reducing displacement. Figure 8 illustrates the connection between displacement and modulus of elasticity. At 0.9 seconds, the displacement measures 0.79 mm at a modulus of 135 MPa and 0.39 mm at a modulus of 400 MPa.

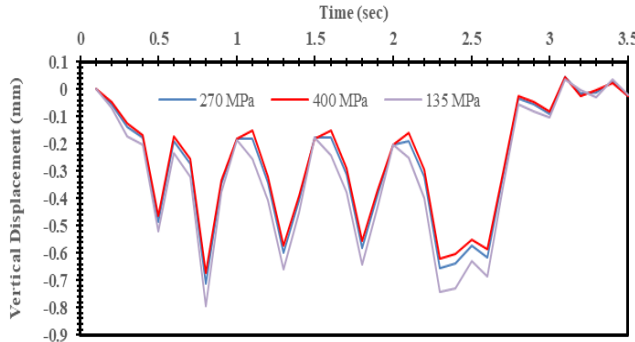


Fig. 8 Vertical displacement of ballast layer with various elastic moduli of ballast

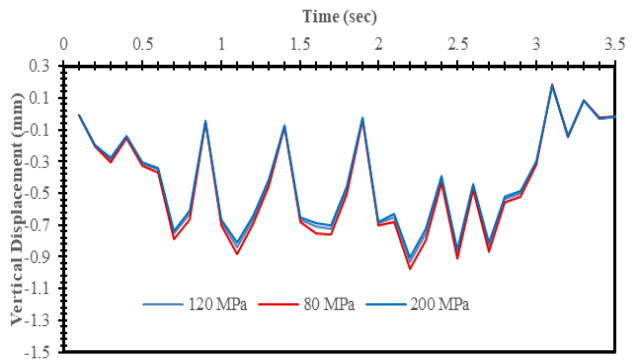


Fig. 11 Vertical displacement of sleeper layer with various elastic moduli of sub-ballast

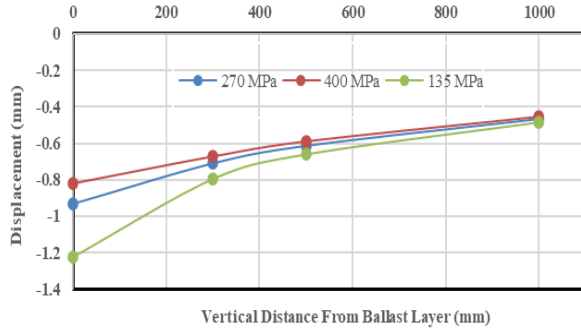


Fig. 9 Vertical displacement from the ballast layer with various elastic moduli of ballast

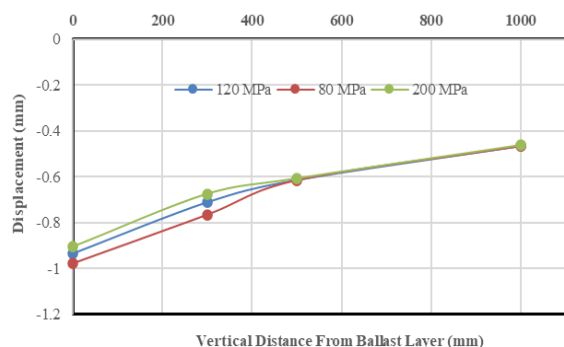


Fig. 12 Vertical displacement from ballast layer with various elastic moduli of sub-ballast

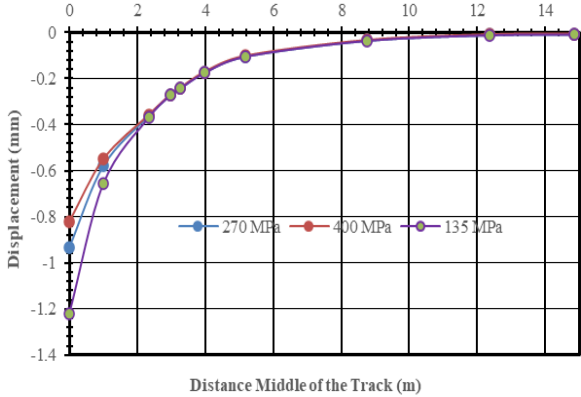


Fig. 10 Horizontal ground vibration from middle of the track different elastic modulus of ballast (in terms of displacement)

Figures 9 and 10 display the variation of displacement in both the vertical and horizontal directions under the dynamic loading conditions. The graph displays the vertical displacement of the railway track extending from the ballast level to the subgrade layer (0-1000 mm). The vertical displacement varies up to 1 meter, but beyond that distance, the displacement is similar regardless of the modulus of elasticity. Figure 10 shows the effect of the modulus of elasticity on vertical displacement due to dynamic loading. Beyond a horizontal distance of 2 meters, the effect of the modulus of elasticity is similar.

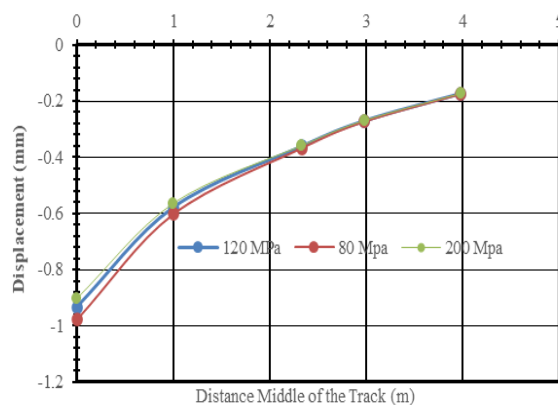


Fig. 13 Horizontal ground vibration from middle of the track with various elastic moduli of sub-ballast (in terms of displacement)

Figures 11 to 13 show the effect of the modulus of elasticity of sub-ballast in the different track layers. The variation of vertical displacement for the variation of the sub-ballast layer's modulus of elasticity is almost the same. Beyond a vertical distance of about 600 mm, the displacement values for all three moduli of elasticity begin to converge. As the vertical distance increases, the displacement decreases. This is because the load dissipates through the ballast and sub-grade layers. The lines show a trend of the downward movement becoming smaller as you move deeper into the ground. By 1000 mm, the displacement for all three cases is

nearly identical at approximately 0.45 mm. This shows that the influence of the sub-grade's stiffness on displacement becomes negligible at greater depths, as the load is sufficiently distributed and the displacement is minimal.

Figure 14 illustrates the bond between vertical displacement and vertical distance from the ballast layer for a railway track. The data is presented for three different moduli of elasticity of the sub-grade layer: 30 MPa, 60 MPa, and 120 MPa. The displacement is largest for the least stiff material (30 MPa, at about -1.02 mm) and smallest for the stiffest material (120 MPa, at about -0.9 mm). This demonstrates that a stiffer sub-grade (higher modulus of elasticity) provides better support and results in less initial deformation.

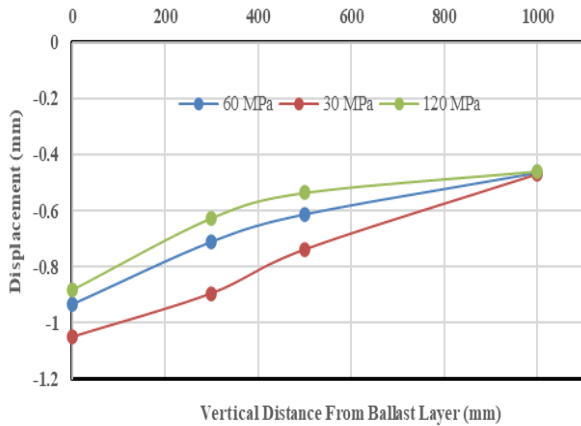


Fig. 14 Vertical displacement from the ballast layer with various elastic moduli of the sub-grade

### 3.2. Linear Regression

Linear regression is carried out to find the relationship between different influencing parameters that affect the ballasted railway track behaviors. The relationship between vertical distance and vertical displacement is shown in Figures 15 to 17 below. A linear equation between Distance and Deflection showed a good fit for all three stress levels, with R-squared values fluctuating from 0.869 to 0.9737.

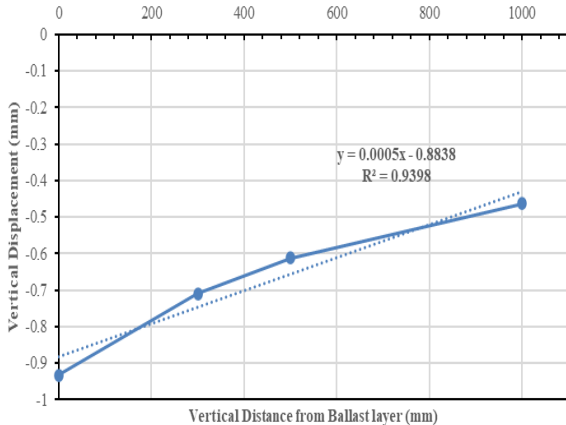


Fig. 15 Linear regression graph between distance and displacement for elastic modulus of 270 MPa

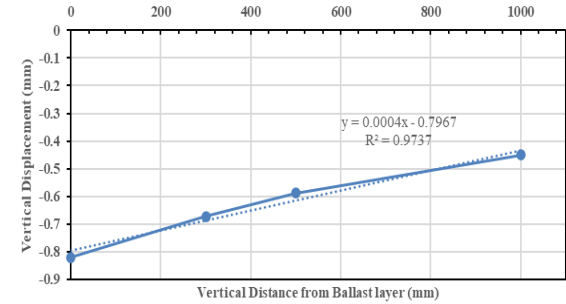


Fig. 16 Linear regression graph between distance and displacement for elastic modulus of 400 MPa

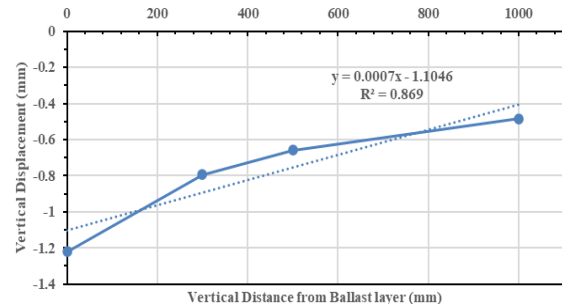


Fig. 17 Linear regression graph between distance and displacement for elastic modulus of 135 MPa

Similarly, a very strong linear relationship is also found between the mean deflection and the Modulus of Elasticity of Ballast (MPa), with an R-squared value of 0.9552, as shown in Figure 18.

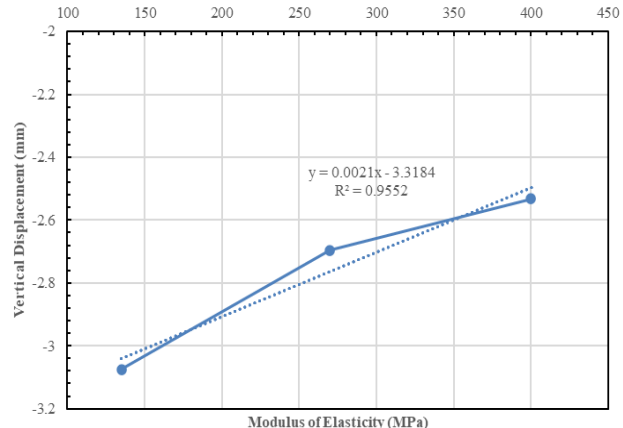


Fig. 18 Linear regression graph between modulus of elasticity and displacement

## 4. Conclusion

This research article uses a validated 3D Finite Element (FE) model to examine the dynamic response of a railway track numerically. The model accurately predicts the track's behaviour under High-Speed Train (HST) movement. Findings from the study show that the overall displacement of the track system is directly affected by the elastic modulus of its constituent materials. The following are the key findings that are summarized below-

- The amplitude of the displacement peaks is influenced by the modulus of elasticity. The stiffer the material, the smaller the range of vertical movement, leading to a more stable track.
- After linear regression analysis, a linear equation between Distance and Deflection showed a good fit for all three stress levels, with R-squared values ranging from 0.869 to 0.9737 and a relationship between the mean deflection and the Modulus of Elasticity of Ballast (MPa), with an R-squared value of 0.9552.
- The study bridges a critical gap in the literature by focusing on the double-track railway system because most of the research concentrates on the single railway track.

## References

- [1] INRIX 2023 Global Traffic Scorecard, INRIX, 2023. [Online]: Available: <https://inrix.com/press-releases/2023-global-traffic-scorecard-uk/>
- [2] Shashank Bharadwaj et al., "Impact of Congestion on Greenhouse Gas Emissions for Road Transport in Mumbai Metropolitan Region," *Transportation Research Procedia*, vol. 25, pp. 3538-3551, 2017. [\[CrossRef\]](#) [\[Google Scholar\]](#) [\[Publisher Link\]](#)
- [3] Amir M. Kaynia, Christian Madshus, and Peter Zackrisson, "Ground Vibration from High-Speed Trains: Prediction and Countermeasure," *Journal of Geotechnical and Geoenvironmental Engineering*, vol. 126, no. 6, pp. 531-537, 2000. [\[CrossRef\]](#) [\[Google Scholar\]](#) [\[Publisher Link\]](#)
- [4] Ernest T. Selig, and John M. Waters, *Track Geotechnology and Substructure Management*, Emerald Publishing Limited, 1994. [\[CrossRef\]](#) [\[Google Scholar\]](#) [\[Publisher Link\]](#)
- [5] Akira Aikawa, "Determination of Dynamic Ballast Characteristics under Transient Impact Loading," *Electronic Journal of Structural Engineering*, vol. 13, no. 1, pp. 17-34, 2013. [\[CrossRef\]](#) [\[Google Scholar\]](#) [\[Publisher Link\]](#)
- [6] Zhongyi Liu, Bin Feng, and Erol Tutumluer, "Effect of Ballast Degradation on Track Dynamic Behavior using Discrete Element Modeling," *Transportation Research Record: Journal of the Transportation Research Board*, vol. 2676, no. 8, pp. 452-462, 2022. [\[CrossRef\]](#) [\[Google Scholar\]](#) [\[Publisher Link\]](#)
- [7] Yahia Alabbasi, and Mohammed Hussein, "Geomechanical Modelling of Railroad Ballast: A Review," *Archives of Computational Methods in Engineering*, vol. 28, no. 3, pp. 815-839, 2021. [\[CrossRef\]](#) [\[Google Scholar\]](#) [\[Publisher Link\]](#)
- [8] Peyman Aela et al., "Influence of Ballast Bulk Density and Loading Conditions on Lateral Resistance of Concrete Sleeper Components," *Proceedings of the Institution of Mechanical Engineers, Part F: Journal of Rail and Rapid Transit*, vol. 237, no. 10, pp. 1284-1293, 2023. [\[CrossRef\]](#) [\[Google Scholar\]](#) [\[Publisher Link\]](#)
- [9] Guixian Liu et al., "Railway Ballast Fouling, Inspection, and Solutions-A Review," *Proceedings of the Institution of Mechanical Engineers, Part F: Journal of Rail and Rapid Transit*, vol. 237, no. 8, pp. 969-982, 2022. [\[CrossRef\]](#) [\[Google Scholar\]](#) [\[Publisher Link\]](#)
- [10] Mohammed A. Alzhrani, Joseph W. Palese, and Allan M. Zarembski, "Assessing the Impact of Sand-Induced Ballast Fouling on Track Stiffness and Settlement," *Geotechnics*, vol. 5, no. 1, pp. 1-30, 2025. [\[CrossRef\]](#) [\[Google Scholar\]](#) [\[Publisher Link\]](#)
- [11] Buddhima Indraratna et al., "Prediction of Resilient Modulus of Ballast under Cyclic Loading using Machine Learning Techniques," *SSRN Electronic Journal*, 2022. [\[CrossRef\]](#) [\[Google Scholar\]](#) [\[Publisher Link\]](#)
- [12] Szabolcs Fischer, "Investigation of the Settlement Behavior of Ballasted Railway Tracks Due to Dynamic Loading," *Spectrum of Mechanical Engineering and Operational Research*, vol. 2, no. 1, pp. 24-46, 2024. [\[CrossRef\]](#) [\[Google Scholar\]](#) [\[Publisher Link\]](#)
- [13] Soumyaranjan Mishra et al., "Use of Recycled Tyre Segments to Enhance the Stability of Ballasted Track by Increased Confinement," *Canadian Geotechnical Journal*, vol. 61, no. 7, pp. 1385-1398, 2023. [\[CrossRef\]](#) [\[Google Scholar\]](#) [\[Publisher Link\]](#)
- [14] G. Castro et al., "Evaluating Environmental Effects on the Structural Behavior of the Railroad Track Subgrade Considering Different Sub-Ballast Design Solutions," *Transportation Geotechnics*, vol. 34, pp. 1-17, 2022. [\[CrossRef\]](#) [\[Google Scholar\]](#) [\[Publisher Link\]](#)
- [15] Iram Lamiya Hoque et al., "Response Analysis of a Ballasted Rail Track Constructed on Soft Soil by 3D Modeling," *Advances in Civil Engineering*, vol. 2023, no. 1, pp. 1-18, 2023. [\[CrossRef\]](#) [\[Google Scholar\]](#) [\[Publisher Link\]](#)
- [16] Weile Qiang et al., "The Use of Recycled Rubber in Ballasted Railway Tracks: A Review," *Journal of Cleaner Production*, vol. 420, pp. 1-43, 2023. [\[CrossRef\]](#) [\[Google Scholar\]](#) [\[Publisher Link\]](#)
- [17] Piyush Punetha, and Sanjay Nimbalkar, "Performance Improvement of Ballasted Railway Tracks for High-Speed Rail Operations," *Challenges and Innovations in Geomechanics*, Turin, Italy, pp. 841-849, 2021. [\[CrossRef\]](#) [\[Google Scholar\]](#) [\[Publisher Link\]](#)
- [18] Meysam Banimahd et al., "Three-Dimensional Modelling of High-Speed Ballasted Railway Tracks," *Proceedings of the Institution of Civil Engineers - Transport*, vol. 166, no. 2, pp. 133-123, 113-123, 2013. [\[CrossRef\]](#) [\[Google Scholar\]](#) [\[Publisher Link\]](#)
- [19] A. El Kacimi et al., "Time Domain 3D Finite Element Modelling of Train-Induced Vibration at High Speed," *Computers & Structures*, vol. 118, pp. 66-73, 2013. [\[CrossRef\]](#) [\[Google Scholar\]](#) [\[Publisher Link\]](#)

## Acknowledgments

The authors wish to express their gratitude to the Department of Civil Engineering at HSTU and at RUET, Bangladesh, for their generous support and provision of facilities.

- [20] Lars Hall, "Simulations and Analysis of Train Induced Ground Vibrations in Finite Element Models," *Soil Dynamics and Earthquake Engineering*, vol. 23, no. 5, pp. 403-413, 2003. [\[CrossRef\]](#) [\[Google Scholar\]](#) [\[Publisher Link\]](#)
- [21] Lars Andersen, and Søren R.K. Nielsen, "Boundary Element Analysis of the Steady-State Response of an Elastic Half-Space to a Moving Force on its Surface," *Engineering Analysis with Boundary Elements*, vol. 27, no. 1, pp. 23-38, 2003. [\[CrossRef\]](#) [\[Google Scholar\]](#) [\[Publisher Link\]](#)
- [22] M. Adam, G. Pfanzl, and G. Schmid, "Two- and Three-Dimensional Modelling of Half-Space and Train-Track Embankment under Dynamic Loading," *Soil Dynamics and Earthquake Engineering*, vol. 19, no. 8, pp. 559-573, 2000. [\[CrossRef\]](#) [\[Google Scholar\]](#) [\[Publisher Link\]](#)
- [23] Xuecheng Bian et al., "Numerical Analysis of Soil Vibrations Due to Trains Moving at Critical Speed," *Acta Geotechnica*, vol. 11, no. 2, pp. 281-294, 2014. [\[CrossRef\]](#) [\[Google Scholar\]](#) [\[Publisher Link\]](#)
- [24] P. Galvin, A. Romero, and J. Domínguez, "Fully Three-Dimensional Analysis of High-Speed Train-Track-Soil-Structure Dynamic Interaction," *Journal of Sound and Vibration*, vol. 329, no. 24, pp. 5147-5163, 2010. [\[CrossRef\]](#) [\[Google Scholar\]](#) [\[Publisher Link\]](#)
- [25] J. O'Brien, and D.C. Rizos, "A 3D BEM-FEM Methodology for Simulation of High-Speed Train Induced Vibrations," *Soil Dynamics and Earthquake Engineering*, vol. 25, no. 4, pp. 289-301, 2005. [\[CrossRef\]](#) [\[Google Scholar\]](#) [\[Publisher Link\]](#)
- [26] Meletetsegwa Gashaw, and Tadahiro Kishida, "Modelling Cyclic Compression of Ballast Aggregates using Boundary Surface Model," *Scientific Reports*, vol. 15, no. 1, pp. 1-14, 2025. [\[CrossRef\]](#) [\[Google Scholar\]](#) [\[Publisher Link\]](#)
- [27] W.L. Lim, and G.R. McDowell, "Discrete Element Modelling of Railway Ballast," *Granular Matter*, vol. 7, no. 1, pp. 19-29, 2005. [\[CrossRef\]](#) [\[Google Scholar\]](#) [\[Publisher Link\]](#)
- [28] Samuel L. Sogin et al., "Comparison of Capacity of Single- and Double-Track Rail Lines," *Transportation Research Record: Journal of the Transportation Research Board*, vol. 2374, no. 1, pp. 111-118, 2013. [\[CrossRef\]](#) [\[Google Scholar\]](#) [\[Publisher Link\]](#)
- [29] Samuel L. Sogin et al., "Analyzing the Transition from Single- to Double-Track Railway Lines with Nonlinear Regression Analysis," *Proceedings of the Institution of Mechanical Engineers, Part F: Journal of Rail and Rapid Transit*, vol. 230, no. 8, pp. 1877-1889, 2016. [\[CrossRef\]](#) [\[Google Scholar\]](#) [\[Publisher Link\]](#)
- [30] Manual of GTS-NX 2013 v1.2: New Experience of Geotechnical Analysis System, MIDAS Company Limited, South Korea, 2013. [Online]. Available: [https://cdn2.hubspot.net/hubfs/3993889/MIDAS%20-%20Documents/GTS\\_NX\\_FABE.pdf](https://cdn2.hubspot.net/hubfs/3993889/MIDAS%20-%20Documents/GTS_NX_FABE.pdf)
- [31] G. Degrande, and L. Schillemans, "Free Field Vibrations during the Passage of a Thalys High-Speed Train at Variable Speed," *Journal of Sound and Vibration*, vol. 247, no. 1, pp. 131-144, 2001. [\[CrossRef\]](#) [\[Google Scholar\]](#) [\[Publisher Link\]](#)
- [32] Nirmal Chandra Roy, and Md. Abu Sayeed, "Investigation into the Behavior of Ballasted Railway Track Foundations through Numerical Analysis," *Journal of Science and Transport Technology*, vol. 5, no. 3, pp. 61-70, 2025. [\[CrossRef\]](#) [\[Google Scholar\]](#) [\[Publisher Link\]](#)